2016

Biomass burning, land-cover change, and the hydrological cycle in Northern sub-Saharan Africa

Charles Ichoku
NASA, Charles.Ichoku@nasa.gov

Luke T. Ellison
NASA

K. Elena Willmot
Vanderbilt University

Toshihisa Matsui
University of Maryland at College Park

Amin K. Dezfuli
USRA

See next page for additional authors

Authors
Charles Ichoku, Luke T. Ellison, K. Elena Willmot, Toshihisa Matsui, Amin K. Dezfuli, Charles K. Gatebe, Jun Wang, Eric M. Wilcox, Jejung Lee, Jimmy Adegoke, Churchill Okonkwo, John Bolten, Frederick S. Policelli, and Shahid Habib

Biomass burning, land-cover change, and the hydrological cycle in Northern sub-Saharan Africa

Environmental Research Letters

LETTER

Biomass burning, land-cover change, and the hydrological cycle in Northern sub-Saharan Africa

Charles Ichoku[1], **Luke T Ellison**[1,2], **K Elena Willmot**[3], **Toshihisa Matsui**[1,4], **Amin K Dezfuli**[1,5], **Charles K Gatebe**[1,5], **Jun Wang**[6,7], **Eric M Wilcox**[8], **Jejung Lee**[9], **Jimmy Adegoke**[9], **Churchill Okonkwo**[10], **John Bolten**[1], **Frederick S Policelli**[1] **and Shahid Habib**[1]

[1] Earth Sciences Division, NASA Goddard Space Flight Center, Greenbelt, MD, USA
[2] Science Systems and Applications Inc., Lanham, MD, USA
[3] Vanderbilt University, Nashville, TN, USA
[4] Earth System Science Interdisciplinary Center (ESSIC), University of Maryland, College Park, MD, USA
[5] Universities Space Research Association (USRA), Columbia, MD, USA
[6] Department of Earth and Atmospheric Sciences, University of Nebraska, Lincoln, NE, USA
[7] Current address: Center for Global and Regional Environmental Research, and Dept. of Chemical and Biochemical Engineering, University of Iowa, USA.
[8] Desert Research Institute, Reno, NV, USA
[9] University of Missouri, Kansas City, MO, USA
[10] Beltsville Center for Climate System Observation, Howard University, Washington, DC, USA

E-mail: Charles.Ichoku@nasa.gov

Keywords: sub-Saharan Africa, biomass burning, water cycle, land cover change, precipitation, fire

OPEN ACCESS

RECEIVED
20 October 2015

REVISED
31 July 2016

ACCEPTED FOR PUBLICATION
19 August 2016

PUBLISHED
14 September 2016

Abstract

The Northern Sub-Saharan African (NSSA) region, which accounts for 20%–25% of the global carbon emissions from biomass burning, also suffers from frequent drought episodes and other disruptions to the hydrological cycle whose adverse societal impacts have been widely reported during the last several decades. This paper presents a conceptual framework of the NSSA regional climate system components that may be linked to biomass burning, as well as detailed analyses of a variety of satellite data for 2001–2014 in conjunction with relevant model-assimilated variables. Satellite fire detections in NSSA show that the vast majority (>75%) occurs in the savanna and woody savanna land-cover types. Starting in the 2006–2007 burning season through the end of the analyzed data in 2014, peak burning activity showed a net decrease of 2–7%/yr in different parts of NSSA, especially in the savanna regions. However, fire distribution shows appreciable coincidence with land-cover change. Although there is variable mutual exchange of different land cover types, during 2003–2013, cropland increased at an estimated rate of 0.28%/yr of the total NSSA land area, with most of it (0.18%/yr) coming from savanna. During the last decade, conversion to croplands increased in some areas classified as forests and wetlands, posing a threat to these vital and vulnerable ecosystems. Seasonal peak burning is anti-correlated with annual water-cycle indicators such as precipitation, soil moisture, vegetation greenness, and evapotranspiration, except in humid West Africa (5°–10° latitude), where this anti-correlation occurs exclusively in the dry season and burning virtually stops when monthly mean precipitation reaches 4 mm d^{-1}. These results provide observational evidence of changes in land-cover and hydrological variables that are consistent with feedbacks from biomass burning in NSSA, and encourage more synergistic modeling and observational studies that can elaborate this feedback mechanism.

1. Introduction

The Northern Sub-Saharan African (NSSA) region is the trans-African latitude zone bounded to the north and south by the Sahara and the Equator, respectively. This region is subjected to intense biomass burning during the dry season each year (e.g. figure 1), contributing 20%–25% of the global total annual carbon emissions from fires (e.g. van der Werf *et al* 2006, 2010, Roberts and Wooster 2008, Schultz *et al* 2008). Over the last several decades, NSSA has suffered from a number of severe drought episodes

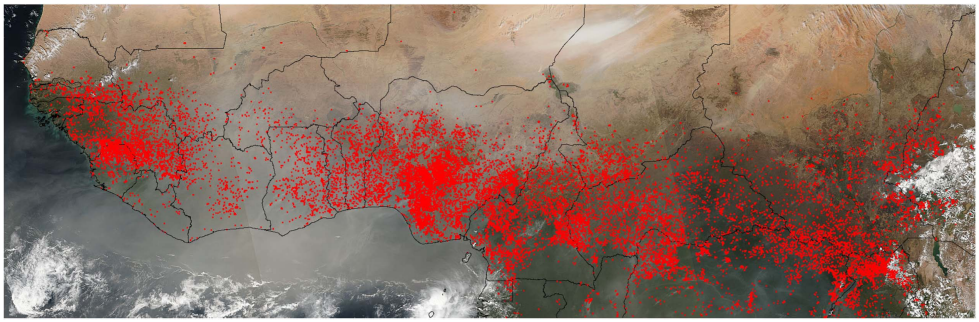

Figure 1. Satellite true color composite image from the Visible Imaging Radiometer Suite (VIIRS) on the Suomi National Polar Partnership (NPP) satellite acquired during three adjoining overpasses across NSSA on 30 January 2016, showing the locations of several thousands of fires (i.e. fire pixels) detected by VIIRS at 750 m spatial resolution marked in red across most of the Northern Sub-Saharan Africa (NSSA). Lake Chad can be seen near the image center, at the Nigeria/Chad boundary, whereas the bright area to its northeast is the Bodélé depression, which is considered to be the largest dust source in the world. Thick gray haze due to the mixing of dust and smoke can be seen across the region especially on the lower left quarter of the image, where it is flowing over the ocean, and appears to interact with the prominent white clouds. (Image courtesy of NASA Earth Observatory—http://earthobservatory.nasa.gov/IOTD/view.php?id=87475).

and associated acute food shortages that have resulted in overwhelming deaths of both people and livestock, particularly in the Sahel zone (i.e. northern NSSA). Among the most severe drought episodes are those that occurred during 1972–1975 and 1984–1985 (e.g. Grove 1986), as well as the more recent 2010–2011 episode in the Horn of Africa (Dutra *et al* 2013, Nicholson 2014). Following the first two episodes, by the 1990s, Lake Chad had shrunk to 5%–10% of its 1963 size of 25 000 km^2 and has still not recovered beyond this limited coverage (e.g. Gao *et al* 2011, Lauwaet *et al* 2012, Lemoalle *et al* 2012).

Previous studies on the possible causes of drought in the Sahel have either focused on sea surface temperature (SST) forcing or land–atmosphere interactions. Several results inferred that regional weather patterns forced by the North Atlantic SST have more influence on the Sahel regional climate than land–atmosphere interactions (Folland *et al* 1986, Giannini *et al* 2003, 2008, Lu and Delworth 2005, Hoerling *et al* 2006, Dai 2011, Nicholson and Dezfuli 2013). There have also been several studies that examined the teleconnection between rainfall variability in the Sahel and variation in SST over the tropical Pacific (Giannini *et al* 2003, 2008, Caminade and Terray 2010). A recent study further suggests that SST fluctuations that result in NSSA drought are strongly influenced by volcanic eruptions in the northern Hemisphere (Haywood *et al* 2013). Simulations of the hydrological impact of land use include those of Charney (1975), Garratt (1993), Xue and Shukla (1993), Xue 1997, Clark *et al* (2001), Taylor *et al* (2002), Li *et al* (2007), and Lebel and Ali (2009), all of which attribute reduced rainfall at least in part to land surface degradation. Specific influences inferred include, for instance: surface albedo (Charney 1975), deforestation (Zheng and Eltahir 1997), vegetation feedback (Claussen *et al* 1999), and soil moisture, with dry soil weakening mature convective systems (Gantner and Kalthoff 2010) and wet soil enhancing the system (Taylor *et al* 2010). In particular, through a number of general circulation model experiments, Taylor *et al* (2002) showed that changes in vegetation in the Sahel can cause substantial reductions in rainfall. Furthermore, Nicholson (2000) and Giannini *et al* (2003, 2008) found that land–atmosphere feedback amplifies variability in the Sahel rainfall resulting from oceanic forcing on the African monsoon. Therefore, improved modeling of the observed variability in precipitation requires knowledge of both SST and land–atmosphere interactions (Wang *et al* 2004).

The role of biomass burning in this phenomenon is not obvious, especially because the dry biomass-burning season (November–April) is out of phase with the rainy season, which occurs mainly from May to October (e.g. Knippertz and Fink 2008). However, a mixture of desert dust and smoke from biomass burning is known to contribute to high aerosol loads in the NSSA atmosphere (e.g. Yang *et al* 2013). Since both the dust and the black carbon from smoke are absorbing aerosols, they can strongly modify the energy balance in the atmosphere and the surface compared with clean conditions (e.g. Chung *et al* 2002, Ramanathan *et al* 2005, Magi *et al* 2008, Lau *et al* 2009, Bollasina *et al* 2011). Details of the aerosol impact on tropospheric and surface energy budgets over land, and hence precipitation and circulation, are related to surface conditions, including land cover, albedo, and soil moisture. For instance, a modeling study involving about a dozen global models coordinated under the Global Land–Atmosphere Coupling Experiment initiative identified regions of strong coupling between soil moisture and precipitation, of which NSSA is the most extensive (Koster *et al* 2004). However, the energy release and aerosol emission from the extensive biomass burning in NSSA are a potential source of perturbation to the system that has not been well addressed.

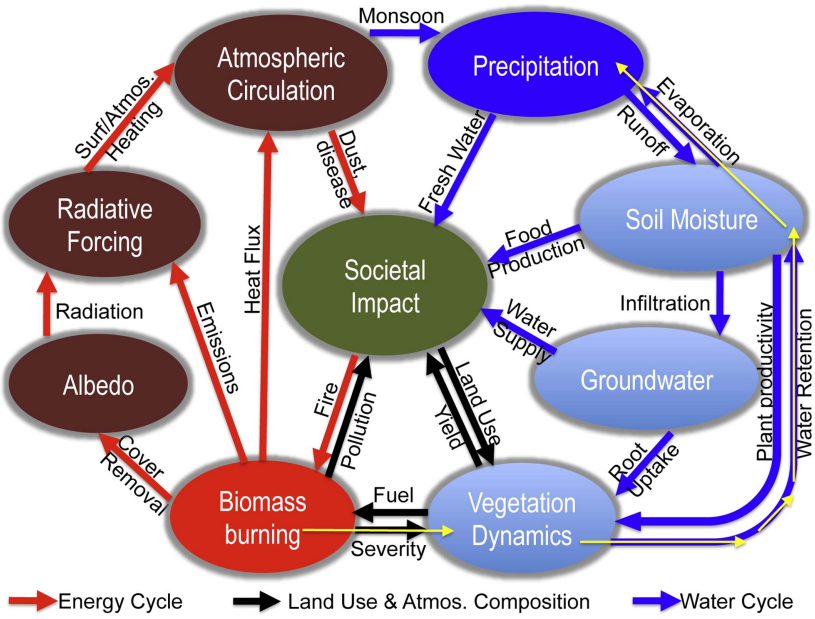

Figure 2. Conceptual schema of the possible links between various environmental phenomena and processes in the Northern Sub-Saharan African (NSSA) region, their repartition into carbon, energy and water cycles, and their relationships to the human society. This reflects the complex nature of the system. Biomass burning and precipitation can be conceived as being diametrically opposite each other, both in character and in season, as their peaks occur approximately six months apart in the NSSA region. The climate component can be perceived as the long-term evolution of this situation. Thin yellow arrows are used to indicate the approximate pathway explored in this study from biomass burning to precipitation, through land-cover changes, vegetation indices, soil moisture, and evapotranspiration.

A growing set of literature is documenting the complex variability and properties of NSSA dust and smoke aerosols (e.g. Yang *et al* 2013, Zhang *et al* 2014). In particular, a recent study provided an observational evidence of smoke aerosol effects on reduction of cloud fraction in that region (Tosca *et al* 2014, 2015). However, there has yet to be a comprehensive study of the relationships between biomass burning and various parameters of the NSSA water cycle. Thus, this paper highlights the recent state and variability of biomass burning, land-cover, and hydrological parameters in a synergistic way. This will help provide a framework for future, more in-depth, studies that will integrate observations into an extensive suite of modeling studies in order to establish how strongly perturbations of terrestrial and biospheric moisture dynamics and regional circulation resulting from biomass burning can eventually affect rainfall, compared to the known impacts of perturbed SST patterns. Section 2 outlines the hypothesis, section 3 the methodology, section 4 the results, while section 5 summarizes the study and provides future perspectives.

2. Hypothesis and scope of study

Given the overwhelming occurrence of biomass burning in NSSA (e.g. van der Werf *et al* 2006, 2010, Ichoku *et al* 2008) and its inherent potential to affect aerosol emissions, surface albedo, vegetation changes, land degradation, deforestation, and surface evapotranspiration, it is reasonable to hypothesize that biomass burning exerts significant impact on the NSSA water cycle directly or indirectly across different spatial and temporal scales. A better understanding of the linkages can only be achieved through a holistic view of the regional land–atmosphere system rather than just individual components.

Figure 2 shows a conceptual schema of the NSSA regional chain of conditions and processes that could be directly or indirectly associated with biomass burning, categorized in terms of how closely they are related to the energy and water cycles, with societal impacts as the focal point. Conceptually, it all starts with human ignition of fires (e.g. Bird and Cali 1998, Dami *et al* 2012), which destroy the vegetation shielding the soil from the intense solar irradiance that characterizes the NSSA region, and modifies the surface albedo (Gatebe *et al* 2014). At the same time, the fire-generated smoke can affect the air quality and can, in conjunction with surface-albedo anomalies, contribute a radiative forcing of the regional climate (e.g. Yang *et al* 2013, Zhang *et al* 2014). Heat fluxes from the fire can affect the atmospheric circulation, which can transport not only dust, but also moisture that can eventually increase or reduce precipitation. The resulting precipitation change has a direct impact on runoff, soil-moisture, infiltration, and groundwater dynamics, whereas the lack of vegetation over the burned areas can lead to an increase in soil erosion and changes in surface water retention properties (e.g. de Wit and Stankiewicz 2006).

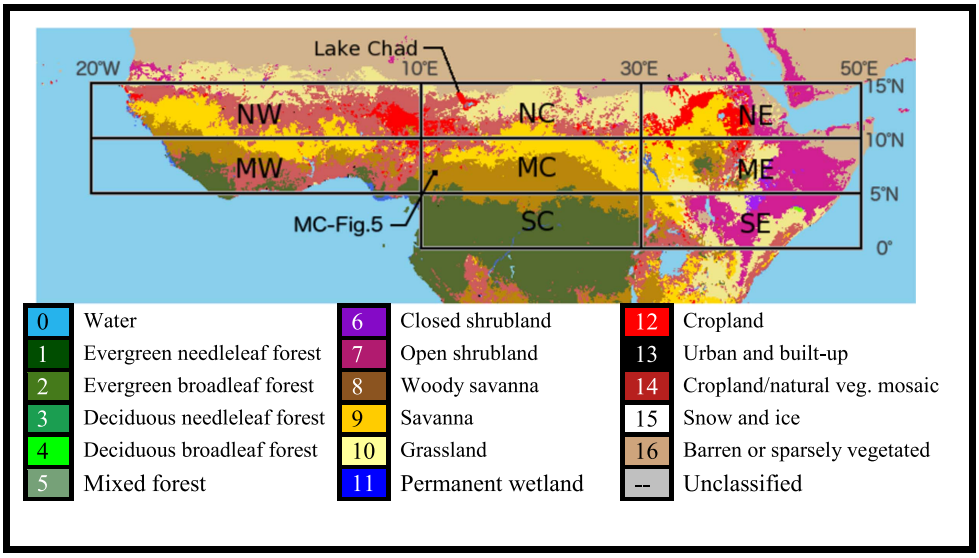

Figure 3. MODIS land cover map of the Northern Sub-Saharan Africa (NSSA) study region based on the international Geosphere–Biosphere Program (IGBP) land cover classification for 2004. Sub-regional blocks artificially delimited for further analysis are identified (horizontally: West, Central, East, and vertically: North, Middle, South), such that labels are composed from the first letters of the vertical and horizontal block coordinates (e.g. NW = north–west and MC = mid-central). The location of lake Chad is shown, whereas that of a small area used to illustrate the detailed dynamics of fire-induced land-cover changes in figure 5 is identified as 'MC-figure 5'.

Spatially, a phenomenon or process in one part of the NSSA region can generate impacts and feedbacks in other parts. Temporally, figure 2 may be visualized as a pseudo annual cycle, with biomass burning and precipitation diametrically across from each other. Over several years or decades, the consequence of the relative interactions and feedbacks of the system components could characterize the nature of the regional climate variability and change, which may influence regional adaptation strategies. Therefore, since biomass burning is an extremely widespread environmental phenomenon in the NSSA region (e.g. figure 1), it is possible that its long-term impacts may include reduction in rainfall, leading to drought.

This study employs data analysis techniques to show some relationships in biomass burning, land-cover change, and other surface and atmospheric parameters associated with the variability of synoptic atmospheric dynamics and hydrological cycle. This pathway is roughly identified using thin yellow arrows in figure 2. It is expected that the results of the analysis performed here will complement other pathways investigated in recent studies (e.g. Yang *et al* 2013, Gatebe *et al* 2014, Tosca *et al* 2014, 2015), and feed into future numerical modeling studies that will unravel the dynamic linkages between these conditions and phenomena at different spatial and temporal scales. Such systems approach will ultimately clarify the indirect pathways from biomass burning to precipitation through the interactions and feedbacks of the related land-use/land-cover, energy-cycle, and water-cycle components, as illustrated in figure 2.

3. Methodology

3.1. Study region characteristics and investigation strategy

The NSSA region (defined in this study as 0°–20°N, 20°W–55°E) features a few prominent land-cover types that go from grasslands in the drier north through a variety of savanna, shrubland, and cropland types as one moves toward the forest in the wetter south (figure 3). There is a relatively equal distribution of the three savanna/grassland land cover types (grasslands, savannas and woody savannas) overall, although the distribution varies significantly between sub-regions. The dominant forest type in the NSSA region is evergreen broadleaf forest (~98% of the regional forest cover). The rainy season in NSSA is clearly distinct from the dry (wildfire) season, with a steep rainfall gradient that goes from $>1000\ \mathrm{mm\ yr^{-1}}$ at latitude 10°N (savanna dominated) down to $<100\ \mathrm{mm\ yr^{-1}}$ at 15°N (grassland dominated), decreasing to trace amounts as the landscape transitions from savanna/grassland (Sahel) land cover type to the arid Sahara Desert.

To facilitate the analysis of conditions and processes that may reflect the unique sub-regional peculiarities of the NSSA region, a large portion of the region (0°–15°N, 20°W–50°E) was divided into nine blocks, of which eight represent land and one represents ocean (figure 3). Regionalization is a typical practice in studying large regions that have spatial heterogeneity, as it facilitates in-depth comparative examination of the sub-regions to characterize the differences in their behaviors with regard to phenomena

of interest (e.g. Dezfuli and Nicholson 2013). In figure 3, the meridional (vertical) boundaries are roughly based on traditional geographical classifications of West, Central, and East Africa, whereas the zonal (horizontal) boundaries are simply located every 5° latitude from 0° to 15°N, to reflect the climatological rainfall gradient. The subdivision could not be based on land-cover types, which change over time, because quantifying their pattern of change due to biomass burning is an objective of this study, and therefore must be conducted within sub-regions with fixed boundaries. The sub-regional blocks used for this study (figure 3) are horizontally identified as: West, Central, East, and vertically identified as: North, Middle, South. The western blocks are each 5° × 30° whereas the rest are 5° × 20°. The block labels are composed from the first letters of the vertical and horizontal block designations (e.g. NW = northern West Africa, MC = middle Central Africa, etc).

3.2. Data resources

There are abundant satellite observations and model-assimilated datasets available for this study. The variables used include: land cover, normalized difference vegetation index (NDVI), fire detection and fire radiative power (FRP), precipitation, soil moisture, and evapotranspiration (ET). The land-cover data are from the MODIS Collection 5 yearly tiled (MCD12Q1) and gridded (MCD12C1) data at 500 m and 0.05° spatial resolutions, respectively (Friedl *et al* 2010). We used the layers based on the International Geosphere–Biosphere Program (IGBP) global vegetation classification scheme. NDVI at 1° resolution (Huete *et al* 2002) were extracted from Collection 5 Terra (MODVI) and Aqua (MYDVI) monthly datasets. Fire detection and FRP data at 1 km spatial resolution were extracted directly from the MODIS Collections 5 and 6 thermal anomalies products (MOD14/MYD14) (Giglio 2013, 2016). Precipitation data at 0.25° × 0.25° spatial resolution and 3-hourly (3B42) and monthly (3B43) temporal resolutions were obtained from the TRMM Multi-satellite Precipitation Analysis version 7 (TMPA v7) products (Huffman *et al* 2007, 2010). Soil moisture data were taken from the European Space Agency's Climate Change Initiative version 2.0 dataset (ESA CCI; Liu *et al* 2012), which combines retrievals from eight different active and passive sensors. Surface evapotranspiration data were obtained from the Global Land Data Assimilation System Version 1 (GLDAS-1) Noah Land Surface Model monthly dataset at 0.25° × 0.25° spatial resolution (Rodell *et al* 2004).

3.3. Data analyses

Analyses of the satellite and model datasets were performed both independently and jointly over each of the eight land blocks (figure 3) for the 14 year (2001–2014) study period, or slightly shorter time periods depending on data availability. The land cover dataset has an overall accuracy of 75% with substantial variability between classes (Friedl *et al* 2010). Based on the recommendation of the data producers, to minimize uncertainty and avoid unnecessary complexity in the analyses that would follow, some of the similar land cover types from the IGBP classification (figure 3) were aggregated to create 10 main land cover categories: water, forest, shrubland, savanna, grassland, wetland, cropland, urban, snow/ice and barren/sparse. Duplicate fire detections that occur at MODIS view angles larger than ±30° were carefully filtered out, so as to mitigate uncertainty in later land-cover change analyses. Since the FRP data are pixel based, in order to generate representative monthly FRP values compatible with the other gridded datasets for a given area, the summation of FRP measurements (in MW units) for each overpass within that area were averaged over the complete number of days in a month, then divided by the land area (km^2), resulting in values expressed in MW km^{-2} or W m^{-2}, which are units of fire radiative energy (FRE) flux.

Previous analyses of fire-induced land cover changes in Africa, particularly in areas dominated by savanna and croplands, encountered large uncertainties due to the relatively coarse resolution of typical satellite observations compared to the small size of burning on the ground (e.g. Ehrlich *et al* 1997). Thus, satellite burned area products were not used in the current study because of their inherent large uncertainties in our study region (e.g. Eva and Lambin 1998, Laris 2005). Instead, to facilitate the analysis of fire-related changes, the individual MODIS fire detections were coupled with the underlying land-cover dataset for the corresponding years. It should be noted that MODIS active fire products are also affected by appreciable uncertainty, especially fire omission due to cloud cover and limited sensitivity to smaller fires (e.g. Schroeder *et al* 2008a, 2008b), which are most prevalent in NSSA.

To facilitate the analysis of potential fire impacts on the water cycle, the relevant variables (FRP, precipitation, soil moisture, evapotranspiration, and NDVI) were analyzed on the basis of the monthly average intensity of each variable and their respective annual integrals or totals. For this part of the study, to avoid inconsistency in jointly analyzing FRP measurements from both Terra and Aqua with other variables, only the FRP acquired from Aqua (with a 1:30 PM local overpass time) were analyzed, as these were acquired closest to the diurnal time of peak burning in the study region (e.g. Ichoku *et al* 2008, Roberts *et al* 2009). The time span for the accumulation of the annual total for each variable was centered on its peak month and extends from one seasonal minimum to the next. Thus, precipitation annual total is accumulated from January to December, soil moisture February–January, evapotranspiration February–January, NDVI February–January, and fires August–July. These

parameters were also separately analyzed only for the dry-season period (November to March) that encompasses the core of the burning activity in all of the NSSA sub-regional blocks. For each of these two categories (full-year and dry-season) inter-annual changes were determined for each of the water-cycle indicators (precipitation, soil moisture, evapotranspiration, and NDVI) and used to generate scatterplots against the afternoon FRE flux values for each of the sub-regional blocks in figure 3, and the associated correlation coefficients were derived. Furthermore, the monthly data, and their respective annual and dry-season integrals were used to generate various types of plots and analyses that provided the results discussed in section 4.

4. Results and discussion

4.1. Fire distribution and land-cover change dynamics

Time-series analysis of the fire activity (represented by FRE flux) during the period of study (2001–2014) showed appreciable progressive increase in the annual peak fire activity until 2006 (especially in the MC block of figure 3) and a steady decrease thereafter. Specifically, the average changes in the annual peak FRE flux (i.e. peak month values) from the 2006/07 season to the 2013/14 season were: NW (−4%/yr), NC (−4%/yr), NE (−7%/yr), MW (−7%/yr), MC (−5%/yr), ME (−2%/yr), SC (−7%/yr), and SE (−3%/yr). This is based on linear least squares fitting to peak month FRE-flux values of all the fire seasons during this period.

To explore possible spatial relationships between fire activity and land-cover dynamics, figure 4 shows the distribution of biomass burning activity and land-cover changes in NSSA during 2003–2013, using the MODIS active fire and land cover data products as described in section 3.2. This particular analysis starts in 2003 because it is the first year the MCD12Q1 product includes full-year input data sets from both the Terra and Aqua platforms, and it ends with the 2012-13 fire season since the last available MCD12Q1 product is for 2013. FRE flux analyses reveal high densities in the savanna/grassland/cropland areas (compare figure 4(a) to 3) and an overall decrease in fire activity since the 2006/07 fire season (figure 4(b)). Detailed analysis of the land-cover datasets show mutual exchanges between different types depending on year. For instance, at a given location, savanna may be converted to cropland in a given year, whereas the opposite happens in a different year. Thus, the coincidence between the areas of intense burning (figures 4(a) and (b) and those of overall land-cover change (figures 4(c), (d) is subtle but still somewhat perceptible. To simplify the interpretation of these complex land-cover change vectors, we focus on croplands, whose expansion is one of the major drivers of burning in NSSA (e.g. Andela and van der Werf 2014). Figures 4(e), (g) and (i) show the distribution of land-cover conversions from savanna, forest, and wetland, respectively to cropland, whereas figures 4(f), (h) and (j) show that these conversions have been on the increase during the last decade (comparing 2006 to 2012), in spite of the overall decreasing trend in burning (figure 4(b)). Table 1 shows a summary of the average annual land-cover changes relative to cropland, which constitutes 18.5% of the total NSSA land area on average. Indeed, croplands have been increasing, in agreement with past studies (e.g. Taylor *et al* 2002, Andela and van der Werf 2014), with an estimated net increase of ∼0.28%/yr of the total NSSA land area. The largest net conversions to cropland come from savannas (0.18%/yr ≈ 24 000 km^2 yr^{-1}) followed by grasslands (0.06%/yr ≈ 8000 km^2 yr^{-1}).

Although it is not easy to show a one-to-one mapping of the cause-and-effect use of fire for land-cover conversion in a region as extensive as NSSA, this phenomenon is illustrated at a relatively perceptible scale using an annual sequence of land-cover maps interspersed by fire detections in the intervening dry seasons (figure 5) in an area near the center of NSSA (MC-figure 5 in figure 3). In this particular case, cropland increased in exchange for savanna from 2006 to 2009, after which it started decreasing and returning to savanna. Coincidentally, starting in the 2009/10 fire season, fire detection increased dramatically in a small patch of forest, which was practically decimated by 2013 and was slowly replaced by cropland and savanna. Similar change patterns were found in several other sampled areas, although these are not shown here for want of space.

An alarming aspect of these results, with particular relevance to water-cycle dynamics, is that, although the average fire activity across NSSA shows a net overall reduction (figure 4(b)), in some cases, there was an increase in the conversion of the more vulnerable land-cover types to cropland, namely forests (e.g. figure 4(h)) and wetlands (e.g. figure 4(j)). This may well be indicative of the indirect effects that these NSSA fires have on the regional water cycle through land cover change. The increasing conversion of the forest land-cover type (e.g. figure 4(h)) is indeed a concern because evergreen forests (as found in NSSA) perform excellent water conservation functions (e.g. Yang *et al* 1992), and the time it takes for a destroyed forest to grow back to its original state is much longer than for savanna or grassland. This is probably one of the major factors contributing to the significant forest loss observed in NSSA from Landsat (30 m resolution) data analysis for the 2000–2012 period (Hansen *et al* 2013). Similarly, wetland is a delicate biome that covers a relatively small percentage of the world's land surface area, and therefore its preservation is important.

In summary, land cover distribution is changing in NSSA, and our analysis support the hypothesis that the

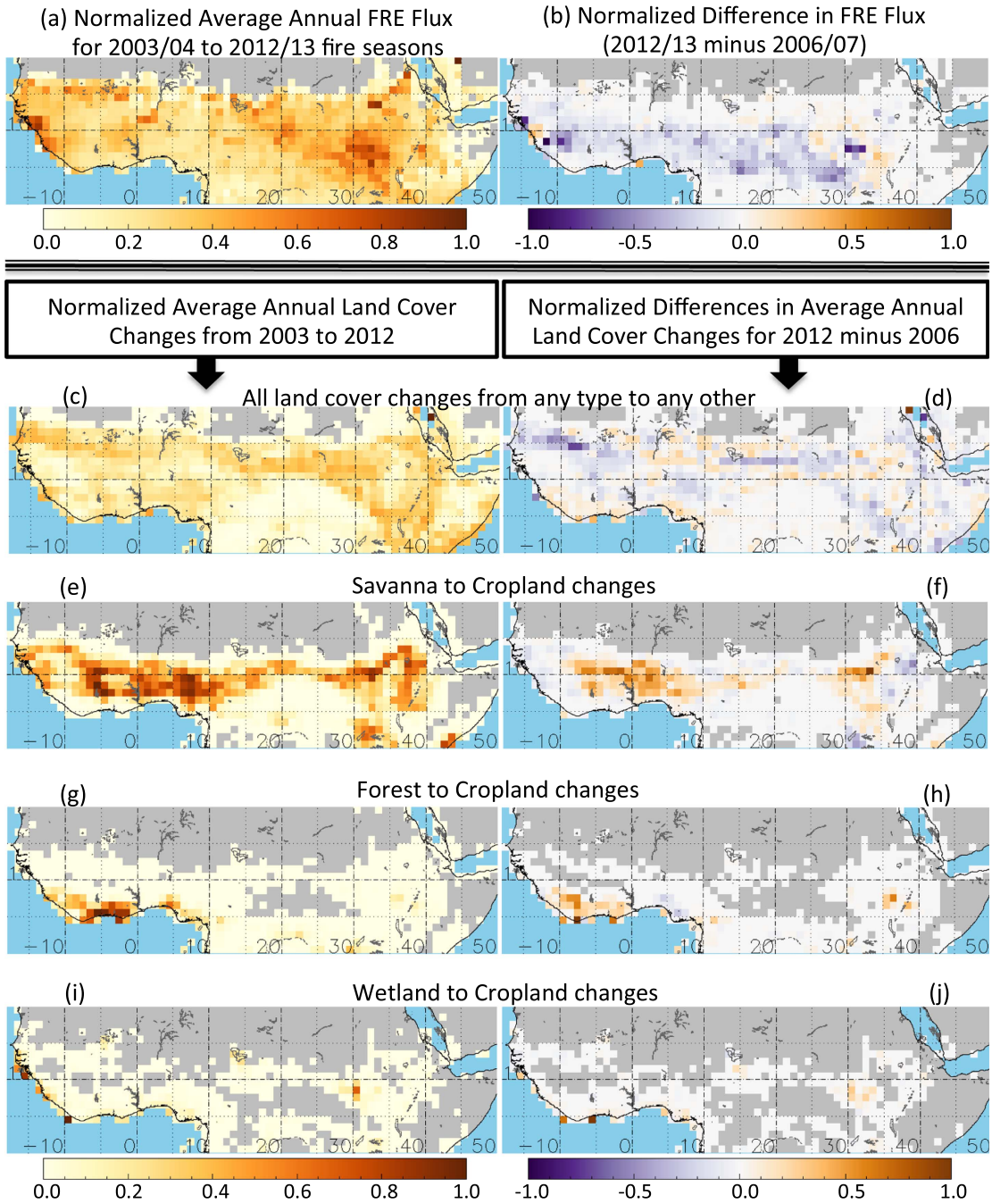

Figure 4. Multi-year (2003–2012) average distributions and changes of fire radiative energy (FRE) flux and land-cover types in the NSSA domain at 1° grid resolution. These analyses are based on MODIS data products: FRE flux from MOD14/MYD14 Collection 6 (fire products at 1 km resolution) and land-cover changes from MCD12Q1 Collection 5 (land cover type classifications at 0.5 km resolution). (a) Average annual FRE flux within each 1° grid, and (b) Difference (2012/13 minus 2006/07) of average annual FRE flux showing a net overall decrease in burning in most parts of NSSA, except in one part of the extreme west coast and some parts of East Africa. For the land-cover changes, the left panels (c), (e), (g) and (i) show the total, savanna-to-cropland, forest-to-cropland, and wetland-to-cropland changes, respectively, whereas the right panels (d), (f), (h) and (j) reflect their respective increase or decrease (2012 minus 2006). All values are linearly scaled from zero to the maximum value on each panel, whereas gray represents the background.

heavy and regular burning practices in NSSA can have a significant effect on the land-cover dynamics. While fires are overall decreasing in the major burning land cover types of savanna/grassland and cropland, certain parts show an increased impact on sensitive land cover types like forest or wetland, which might have some serious ecological and hydrological implications.

4.2. Potential relationships between biomass burning and the water cycle

The potential relationships of biomass burning activity to the water cycle has been explored by analyzing how changes in biomass burning relate to those of relevant water-cycle indicators, including soil moisture, NDVI, evapotranspiration, and precipitation. A general linear least squares regression analysis shows appreciable

Table 1. Summary of the average annual land-cover fraction and conversion rates (%/yr) to and from the ***cropland*** type over the period of 2003 to 2013 relative to the total NSSA land area, and the net increase in cropland.

Land cover types	Fraction of total land	To cropland	From cropland	Net increase in cropland (*To—from*)
Forest	10.2%	0.18%	0.18%	0.00%
Shrubland	8.2%	0.29%	0.28%	0.02%
Savanna	22.3%	1.54%	1.36%	0.18%
Grassland	12.1%	1.46%	1.40%	0.06%
Wetland	0.6%	0.014%	0.016%	0.00%
Cropland	18.5%	15.24%	15.24%	0.00%
Barren	28.0%	0.081%	0.064%	0.02%
Totals	99.9%	3.6%	3.3%	0.28%

(mostly negative) correlation between inter-annual changes in annual average afternoon FRE flux and inter-annual changes in the annual averages or integrals of a set of water-cycle indicators in NSSA and its sub-regional blocks (figure 6(a)). Inter-annual changes are used as a way to minimize the effects of quantitative biases and uncertainties, which can vary substantially for certain water-cycle parameters depending on data source (e.g. Rodell *et al* 2011). Similar correlations between FRE flux and the water-cycle parameters were also calculated for the dry-season (set as November–March) when fires occur (figure 6(b)).

For the full annual correlations (figure 6(a)), the inter-annual change in afternoon FRE flux from one year (August–July) to the next is paired with the inter-annual changes in the different water-cycle parameters between their respective pairs of the next closest annual cycles (January–December for precipitation and February–January for the other parameters). For example, the change of afternoon FRP flux from the August 2002–July 2003 season to the August 2003–July 2004 season is paired with the change of precipitation from the January–December 2003 season to the January–December 2004 season. This was done to ensure that changes in fire activity lead (with some overlap) those of precipitation, soil moisture, NDVI, and evapotranspiration, so as to establish a basis for the attribution of the changes in these water cycle parameters, at least in part, to the biomass burning effects. Most of the significant correlations are negative especially along the northern blocks (NW, NC, NE), suggesting that the more severe the fire season in these northern blocks, the more severe the decrease in these water-cycle indicators, particularly soil moisture and NDVI, in the following rainy season. The main exception is the MW block, where it would seem that the greater the change in seasonal mean afternoon FRE flux, the greater the change in the seasonal mean NDVI during the subsequent rainy season. This might be because much of the burning in this MW block seems to be for the conversion of savanna (and, to a lesser extent, forest) to cropland (figures 4(e)–(h)), thereby producing newer and perhaps overall greener vegetation than savanna.

On the other hand, when only the dry season (in this case, November–March) inter-annual changes in these water-cycle indicators are regressed against the concurrent inter-annual change in afternoon FRE flux, they all result in significant negative correlations in the MW block (figure 6(b)). There is a similar negative precipitation change correlation with afternoon FRE flux in the NE block and the NSSA overall. Worth noting also is the significant positive correlation of some of the water-cycle indicators (NDVI and evapotranspiration) against afternoon FRE flux during the dry season (figure 6(b)) in the NC block that contains Lake Chad (figure 3), suggesting that increase in burning coincides with increase in vegetation greenness and evapotranspiration, which is consistent with burning for irrigated agriculture during the dry season probably within the floodplains of Lake Chad and its tributaries, as indicated by the appreciable and relatively increased conversion of wetlands to croplands (figures 4(i) and (j)).

4.3. Biomass burning and the water cycle during the dry season

The potential link of biomass burning to the water cycle parameters during the dry (fire) season (November–March) is further explored in each NSSA sub-regional block by comparing the time-series of afternoon FRE flux against total precipitation and evapotranspiration for the same time period (figure 7). The MC block obviously shows the highest burn activity, with an apparent decrease over the last decade (figure 4(b)). Overall, it appears that blocks with relatively high burn activity (FRE flux $>0.02\ \mathrm{W\ m^{-2}}$ i.e. MW and MC) show a much higher evapotranspiration over precipitation. However, with the exception of the northern blocks where there is little to no precipitation during the biomass-burning season, afternoon FRE flux appears to show some inverse relationships with the off-season precipitation and evapotranspiration in some blocks, of which the most prominent is the MW block (see also figure 6(b)), where some sharp peaks in burning coincide with sharp dips in dry-season precipitation and vice versa (figure 7).

Therefore, a concentrated effort focused on the MW block is pursued in an attempt to understand the interactions between the burning and water cycle better. A scatterplot of afternoon FRE flux against precipitation for the MW block shows that burning has indeed an inverse (albeit nonlinear) relationship with precipitation, but stops or becomes insignificant when the average monthly precipitation stays above $4\ \mathrm{mm\ d^{-1}}$ (figure 8). However, as the seasonal transition month in MW, April stands out with its points

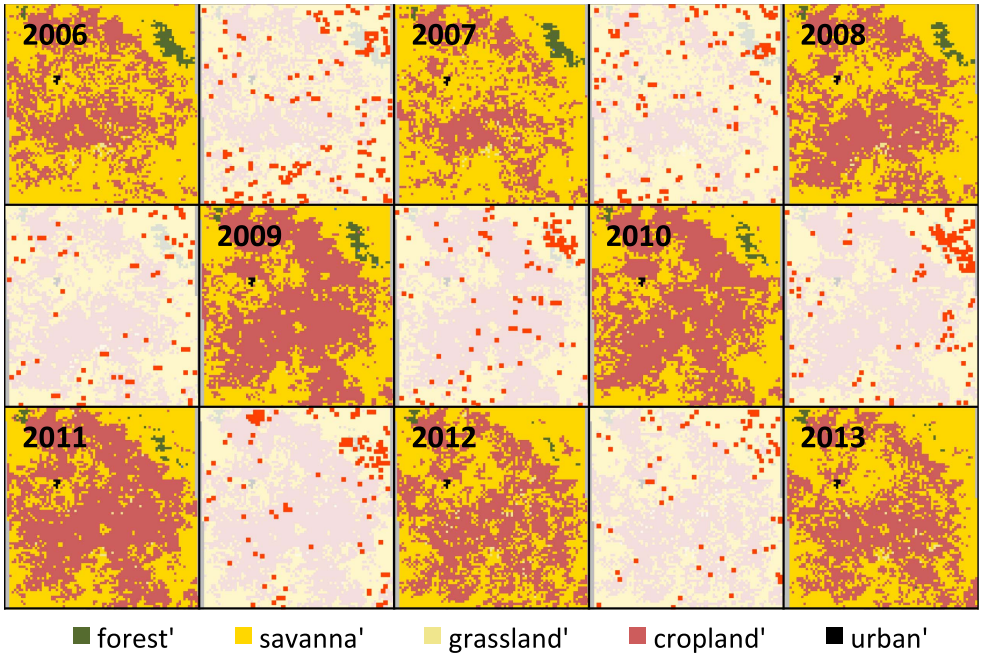

Figure 5. Annual sequence of land-cover distributions from 2006 to 2013 in a small area ('MC-figure 5' in figure 3) bounded by 6.74°–7.09°N, 11.02°–11.36°E. Between consecutive years, Terra- and Aqua-MODIS fire pixels (red dots) detected during the intervening fire seasons are highlighted over the significantly saturated land-cover panel of the leading year, to show the land covers potentially burning. Cropland density seems to increase from 2003 until 2009, after which it started decreasing slowly. A patch of forest can be seen near the top right corner of the panels during those years. However, starting in the 2009/2010 fire season, fire detection increased dramatically in that patch of forest, which was practically decimated by 2013 and slowly replaced by cropland and savanna.

portraying a quasi-linear distribution suggestive of a positive correlation (figure 8), which could be indicative of precipitation enhancement due to biomass burning. This interpretation has substantial agreement with Huang *et al* (2009, figure 3) who found that aerosols (including both dust and smoke) in West Africa may be responsible for precipitation enhancement over land and suppression over ocean. The current study has gone a step further by isolating a possible biomass-burning enhancement of precipitation in humid West Africa (i.e. block MW) during the month of April.

These analyses suggest the need for a more detailed study of the mechanisms governing the biomass burning enhancement/suppression/delay of rainfall in NSSA. The potential effects of such mechanisms may include the lengthening of the dry season and increased perturbation of the seasonal precipitation patterns, whose human dimension is important, given the very high population density/growth in most of NSSA (e.g. Ezeh *et al* 2012). Chauvin *et al* (2012) reports that although agricultural production has been increasing slightly in SSA overall, it has certainly not kept up with the population increase, and that the per capita food consumption has been decreasing rather steadily since the 1970s with a slight increase during the 2000s. Detailed studies that can unravel these mechanisms will require strategic synergism between data analysis and a variety of modeling experiments.

5. Conclusions and outlook

The intense biomass burning activity across the NSSA region has significant implications for changes in the regional land cover, water cycle, and climate. This study has enabled a description of recent (2001–2014) variability in several important land-cover and water-cycle variables in relation to biomass burning, thereby offering some insights into their potential couplings. Starting in the 2006/2007 burning season through the end of the analyzed data in 2014, peak burn activity steadily decreased by 2–7%/year in different parts of the NSSA region. Incidentally, during the same period, in some cases, fire-related land-cover changes have increased in the more vulnerable land-cover types that were traditionally less burned, such as forests and wetlands. Although changes were also observed in precipitation, soil moisture, NDVI, and surface evapotranspiration in certain parts of the region, it is not easy to clearly establish a generalized cause-and-effect relationship between biomass burning and these hydrological cycle indicators mainly because of the difference in the seasonality between them.

However, based on precipitation data covering the period of 2001–2014, it is established that, during the rainy season, average monthly precipitation in humid West Africa (MW block) always exceeds 4 mm d^{-1}. This value, if used for model parameterization, may have some implications on predicting how precipitation intensity and variability could affect or be affected by biomass burning in the future. Since precipitation

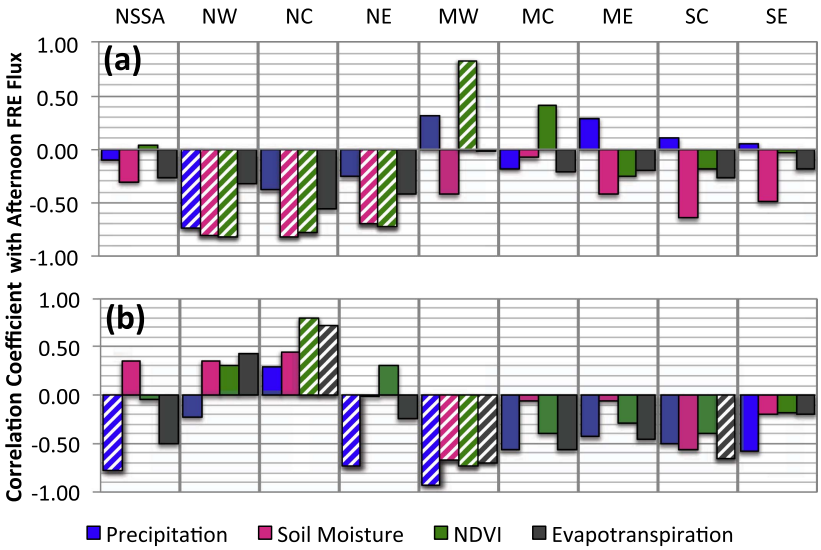

Figure 6. Correlation coefficients (r) between interannual changes in afternoon biomass burning (represented by year-to-year changes in annual average FRE flux derived from Aqua-MODIS FRP measurements at ~1:30 PM local time overpass for 2001–2014) and those of certain indicators of the water cycle and environmental conditions for NSSA and its sub-regional blocks, both on the basis of: (a) integration or averaging through the full-year cycle and, (b) integration or averaging through only the dry-season (November–March). The striped bars indicate correlation coefficient values that are significant at the 95% confidence level. The data sources are: precipitation (TRMM–TMPA), soil moisture (ESA–CCI), NDVI (MODIS-Terra), and evapotranspiration (GLDAS).

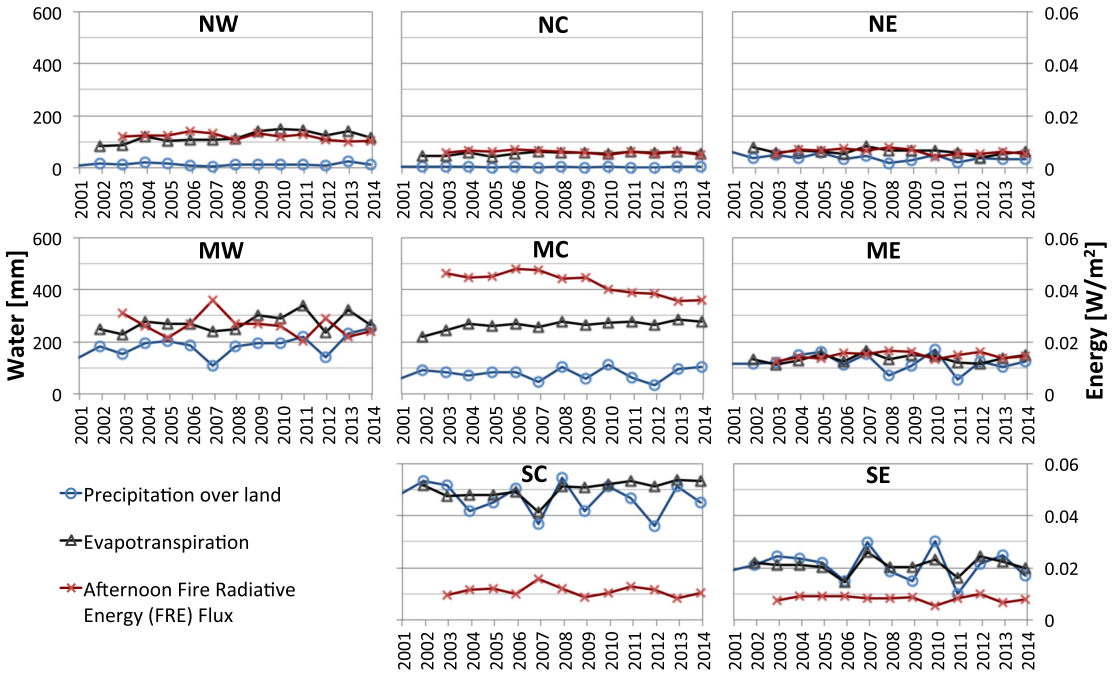

Figure 7. Time series of dry (fire) season (November–March) afternoon FRE flux from MODIS-Aqua, precipitation from TRMM, and evapotranspiration from GLDAS for the NSSA sub-regional blocks. The left Y-axis (Water (mm)) represents precipitation and evapotranspiration, whereas the right Y-axis (Energy (W m^{-2})) represents the FRE flux.

itself is affected by atmospheric circulation, surface state, and aerosol loading through nonlinear physical processes (e.g. Pielke *et al* 2007), such conditions could eventually produce an adverse feedback to agricultural activities. Thus, if future monthly precipitation remains below 4 mm d^{-1} at the onset of the rainy season, it is possible that regional farmers could continue burning the biomass to prepare their farmland, with potentially severe implications for the regional water cycle and climate.

Although these results are quite appealing, further details of the time-lapse and sensitivity of the seasonal precipitation to fire-induced surface changes, energy release, and emissions in NSSA and its sub-regions are complex to elaborate based only on the data analysis performed here. Such processes need to be explored

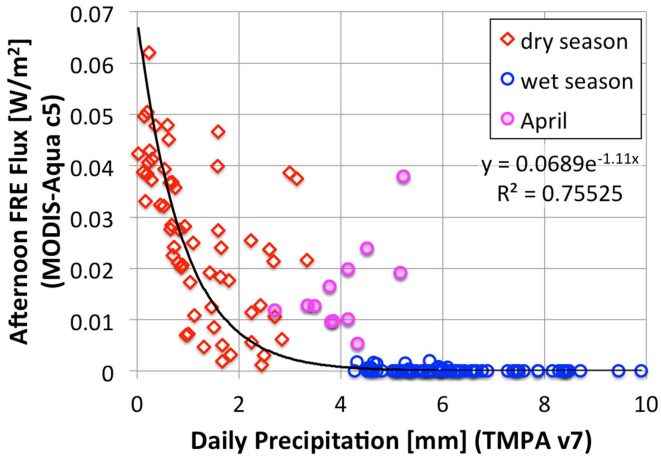

Figure 8. MW block (see figure 3) scatterplot of afternoon FRE flux against precipitation showing the demarcation between the rainy (May–October) and dry (November–March) season to be ~4 mm d^{-1}, with the transition month of April standing out.

further using regional climate models and additional data sets, with a view to developing a comprehensive understanding of the phenomena and connections as laid out in the original conceptual framework (figure 2). Future effort should involve an extensive suite of modeling studies that will integrate observations. These should be simulations of 10 year or longer durations where a control simulation is compared with experimental runs with perturbed boundary conditions or perturbed forcing. Experiments should test the sensitivity of the circulation and precipitation patterns to: (i) land-cover-change and surface albedo perturbations due to biomass burning based on observations; (ii) lower tropospheric heating by smoke aerosol absorption; (iii) surface radiative cooling owing to aerosol scattering and absorption; (iv) perturbed cloud cover owing to aerosol modification of cloud amount; and (v) perturbed soil moisture based on observed variability. A key question that can be addressed through these experiments is how strong an impact each of these perturbations has on the circulation and rainfall compared to the established impact of perturbed SST patterns.

Acknowledgments

This research was fully funded by NASA under its Research Opportunities in Space and Earth Sciences (ROSES)—2009 and 2013 Interdisciplinary Studies (IDS) Program (Dr Jack Kaye, Earth Science Research Director) through the Radiation Sciences Program managed by Dr Hal Maring. We also appreciate the efforts of providers of the large diversity of data products used for this study from various satellite sensors and global models.

References

Andela N and van der Werf G R 2014 Recent trends in African fires driven by cropland expansion and El Nino to La Nina transition *Nat. Clim. Change* **4** 791–5

Bird M I and Cali J A 1998 A million-year record of fire in sub-Saharan Africa *Nature* **394** 767–9

Bollasina M, Ming Y and Ramaswamy V 2011 Anthropogenic aerosols and the weakening of the South Asian summer monsoon *Science* **334** 502–5

Caminade C and Terray L 2010 Twentieth century Sahel rainfall variability as simulated by the ARPEGE AGCM, and future changes *Clim. Dyn.* **35** 75–94

Charney J G 1975 Dynamics of deserts and drought in the Sahel *Q. J. R. Meteorol. Soc* **101** 193–202

Chauvin N D, Mulangu F and Porto G 2012 Food production and consumption trends in Sub-Saharan Africa: prospects for the transformation of the agricultural sector *Working Paper, United Nations Development Programme, Regional Bureau for Africa*WP 2012–011 (http://undp.org/content/dam/rba/docs/Working%20Papers/Food%20Production%20and%20Consumption.pdf)

Chung C E, Ramanathan V and Kiehl J T 2002 Effects of the South Asian absorbing haze on the northeast monsoon and surface–air heat exchange *J. Clim.* **15** 2462–76

Claussen M, Kubatzki C, Brovkin V, Ganopolski A, Hoelzmann P and Pachur H J 1999 Simulation of an abrupt change in Saharan vegetation in the mid-Holocene *Geophys. Res. Lett.* **26** 2037–40

Clark D B, Xue Y K, Harding R J and Valdes P J 2001 Modeling the impact of land surface degradation on the climate of tropical North Africa *J. Clim.* **14** 1809–22

Dai A 2011 Drought under global warming: a review *Wiley Interdiscip. Rev.: Clim. Change* **2** 45–65

Dami A, Ayuba H K and Bila M 2012 Analysis of the relationship between wildfire occurrences and population trend within the shores of lake Chad basin using geoinformation *J. Geographys. Geol.* **4** 49–55

de Wit M and Stankiewicz J 2006 Changes in surface water supply across Africa with predicted climate change *Science* **311** 1917–21

Dezfuli A K and Nicholson S E 2013 The relationship of rainfall variability in western equatorial Africa to the tropical oceans and atmospheric circulation: II. The boreal autumn *J. Clim.* **26** 66–84

Dutra E, Magnunson L, Wetterhall F, Cloke H L, Balsamo G, Boussetta S and Pappenberger F 2013 The 2010–11 drought

in the Horn of Africa in the ECMWF reanalysis and seasonal forecast products *Int. J. Climatol.* **33** 1720–9
Ehrlich D, Lambin E F and Malingreau J P 1997 Biomass burning and broad-scale land-cover changes in Western Africa *Remote Sens. Environ.* **61** 201–9
Eva H and Lambin E F 1998 Remote sensing of biomass burning in tropical regions: sampling issues and multisensor approach *Remote Sens. Environ.* **64** 292–315
Ezeh A C, Bongaarts J and Mberu B 2012 Family planning: I. Global population trends and policy options *Lancet* **380** 142–8
Folland C K, Palmer T N and Parker D 1986 Sahel rainfall and worldwide sea temperature 1901–85 *Nature* **320** 602–87
Friedl M A, Sulla-Menashe D, Tan B, Schneider A, Ramankutty N, Sibley A and Huang X 2010 MODIS collection 5 global land cover: algorithm refinements and characterization of new datasets *Remote Sens. Environ.* **114** 168–82
Gantner L and Kalthoff N 2010 Sensitivity of a modelled life cycle of a mesoscale convective system to soil conditions over West Africa *Q. J. R. Meteorol. Soc.* **137** 471–82
Gao H, Bohn T J, Podest E, McDonald K C and Lettenmaier D P 2011 On the causes of the shrinking of Lake Chad *Environ. Res. Lett.* **6** 034021
Garratt J R 1993 Sensitivity of climate simulations to land-surface and atmospheric boundary-layer treatments—a review *J. Clim.* **6** 419–49
Gatebe C K, Ichoku C M, Poudyal R, Román M O and Wilcox E 2014 Surface albedo darkening from wildfires in Northern Sub-Saharan Africa *Environ. Res. Lett.* **9** 065003
Giannini A, Biasutti M and Verstraete M M 2008 A climate model-based review of drought in the Sahel: desertification, the re-greening and climate change *Glob. Planet. Change* **64** 119–28
Giannini A, Saravanan R and Chang P 2003 Oceanic forcing of Sahel rainfall on interannual to interdecadal time scales *Science* **302** 1027–30
Giglio L 2013 MODIS Collection 5 Active Fire Product User's Guide Version 2.5 (http://modis-fire.umd.edu/files/MODIS_Fire_Users_Guide_2.5.pdf)
Giglio L, Schroeder W and Justice C O 2016 The collection 6 MODIS active fire detection algorithm and fire products *Remote Sens. Environ.* **178** 31–41
Grove A T 1986 The State of Africa in the 1980s *Geogr. J.* **152** 193–203
Hansen M C *et al* 2013 High-resolution global maps of 21st-century forest cover change *Science* **342** 850–3
Haywood J M, Jones A, Bellouin N and Stephenson D 2013 Asymmetric forcing from stratospheric aerosols impacts Sahelian rainfall *Nat. Clim. Change* **3** 660–5
Hoerling M, Hurrell J, Eischeid J and Phillips A 2006 Detection and attribution of twentieth-century Northern and Southern African rainfall change *J. Clim.* **19** 3989–4008
Huang J, Zhang C and Prospero J M 2009 African aerosol and large-scale precipitation variability over West Africa *Environ. Res. Lett.* **4** 015006
Huete A, Didan K, Miura T, Rodriguez E P, Gao X and Ferreira L G 2002 Overview of the radiometric and biophysical performance of the MODIS vegetation indices *Remote Sens. Environ.* **83** 195–213
Huffman G J, Adler R F, Bolvin D T and Nelkin E J 2010 The TRMM multi-satellite precipitation analysis (TMPA) *Satellite Rainfall Applications for Surface Hydrology* (Netherlands: Springer) pp 3–22
Huffman G J, Bolvin D T, Nelkin E J, Wolff D B, Adler R F, Gu G, Hong Y, Bowman K P and Stocker E F 2007 The TRMM multisatellite precipitation analysis (TMPA): quasi-global, multiyear, combined-sensor precipitation estimates at fine scales *J. Hydrometeorol.* **8** 38–55
Ichoku C, Giglio L, Wooster M J and Remer L A 2008 Global characterization of biomass-burning patterns using satellite measurements of fire radiative energy *Remote Sens. Environ.* **112** 2950–62
Knippertz P and Fink A H 2008 Dry-season precipitation in tropical West Africa and its relation to forcing from the extratropics *Mon. Weather Rev.* **136** 3579–96
Koster R D *et al* 2004 Regions of strong coupling between soil moisture and precipitation *Science* **305** 1138–40
Laris P S 2005 Spatiotemporal problems with detecting and mapping mosaic fire regimes with coarse-resolution satellite data in savanna environments *Remote Sens. Environ.* **99** 412–24
Lau K M, Kim K M, Sud Y C and Walker G K 2009 A GCM study of the response of the atmospheric water cycle of West Africa and the Atlantic to Saharan dust radiative forcing *Ann. Geophys.* **27** 4023–37
Lauwaet D, van Lipzig N P M, Van Weverberg K, De Ridder K and Goyens C 2012 The precipitation response to the desiccation of Lake Chad *Q. J. R. Meteorol. Soc.* **138** 707–19
Lebel T and Ali A 2009 Recent trends in the Central and Western Sahel rainfall regime (1990-2007) *J. Hydrol.* **375** 52–64
Lemoalle J, Bader J–C, Leblanc M and Sedick A 2012 Recent changes in Lake Chad: observations, simulations and management options (1973–2011) *Glob. Planet. Change* **80-81** 247–54
Li K Y, Coe M T, Ramankutty N and De Jong R 2007 Modeling the hydrological impact of land-use change in West Africa *J. Hydrol.* **337** 258–68
Liu Y Y, Dorigo W A, Parinussa R M, de Jeu R A M, Wagner W, McCabe M F, Evans J P and van Dijk A I J M 2012 Trend-preserving blending of passive and active microwave soil moisture retrievals *Remote Sens. Environ.* **123** 280–97
Lu J and Delworth T L 2005 Oceanic forcing of the late 20th century Sahel drought *Geophys. Res. Lett.* **32** L22706
Magi B I, Fu Q, Redemann J and Schmid B 2008 Using aircraft measurements to estimate the magnitude and uncertainty of the shortwave direct radiative forcing of southern African biomass burning aerosol *J. Geophys. Res.* **113** D05213
Nicholson S 2000 Land surface processes and Sahel climate *Rev. Geophys.* **38** 117–39
Nicholson S 2014 The predictability of rainfall over the greater horn of Africa: I. Prediction of seasonal rainfall *J. Hydrometeorol.* **15** 1011–27
Nicholson S E and Dezfuli A K 2013 The relationship of rainfall variability in western equatorial Africa to the tropical oceans and atmospheric circulation: I. The boreal spring *J. Clim.* **26** 45–65
Pielke R A, Adegoke J O, Chase T N, Marshall C H, Matsui T and Nigygi D 2007 A new paradigm for assessing the role of agriculture in the climate system and in climate change *Agric. Forest Meteorol.* **142** 234–54
Ramanathan V, Chung C, Kim D, Bettge T, Buja L, Kiehl J T, Washington W M, Fu Q, Sikka D R and Wild M 2005 Atmospheric brown clouds: impacts on South Asian climate and hydrological cycle *Proc. Natl Acad. Sci.* **102** 5326–33
Roberts G, Wooster M J and Lagoudakis E 2009 Annual and diurnal African biomass burning temporal dynamics *Biogeosciences* **6** 849–66
Roberts G J and Wooster M J 2008 Fire detection and fire characterization over Africa using meteosat SEVIRI *IEEE Trans. Geosci. Remote Sens.* **46** 1200–18
Rodell M, Famiglietti J S, Chen J, Seneviratne S I, Viterbo P, Holl S and Wilson C R 2004 Basin scale estimates of evapotranspiration using GRACE and other observations *Geophys. Res. Lett.* **31** L20504
Rodell M, McWilliams E B, Famiglietti J S, Beaudoing H K and Nigro J 2011 Estimating evapotranspiration using an observation based terrestrial water budget *Hydrol. Process.* **25** 4082–92
Schroeder W, Prins E, Giglio L, Csiszar I, Schmidt C, Morisette J and Morton D 2008a Validation of GOES and MODIS active fire detection products using ASTER and ETM plus data *Remote Sens. Environ.* **112** 2711–26
Schroeder W, Ruminski M, Csiszar I, Giglio L, Prins E, Schmidt C and Morisette J 2008b Validation analyses of an operational fire monitoring product: the hazard mapping system *Int. J. Remote Sens.* **29** 6059–66
Schultz M G, Heil A, Hoelzemann J J, Spessa A, Thonicke K, Goldammer J G, Held A C, Pereira J M C and van het Bolscher M 2008 Global wildland fire emissions from 1960 to 2000 *Global Biogeochem. Cycles* **22** GB2002

Taylor C M, Lambin E F, Stephenne N, Harding R J and Essery R L H 2002 The influence of land use change on climate in the Sahel *J. Clim.* **15** 3615–29

Taylor C M, Harrisa P P and Parkerb D J 2010 Impact of soil moisture on the development of a sahelian mesoscale convective system: a case-study from the AMMA special observing period *Q. J. R. Meteorol. Soc.* **136** 456–70

Tosca M G, Diner D J, Garay M J and Kalashnikova O V 2014 Observational evidence of fire-driven reduction of cloud fraction in tropical Africa *J. Geophys. Res. Atmos.* **119** 8418–32

Tosca M G, Diner D J, Garay M J and Kalashnikova O V 2015 Human-caused fires limit convection in tropical Africa: first temporal observations and attribution *Geophys. Res. Lett.* **42** 6492–501

van der Werf G R, Randerson J T, Giglio L, Collatz G J, Kasibhatla P S and Arellano A F 2006 Interannual variability in global biomass burning emissions from 1997 to 2004 *Atmos. Chem. Phys.* **6** 3423–41

van der Werf G R, Randerson J T, Giglio L, Collatz G J, Mu M, Kasibhatla P S, Morton D C, DeFries R S, Jin Y and van Leeuwen T T 2010 Global fire emissions and the contribution of deforestation, savanna, forest, agricultural, and peat fires (1997–2009) *Atmos. Chem. Phys.* **10** 11707–35

Wang G, Eltahir E A B, Foley J A, Pollard D and Levis S 2004 Decadal variability of rainfall in the Sahel: results from the coupled GENESIS-IBIS atmosphere-biosphere model *Clim. Dyn.* **22** 625–37

Xue Y 1997 Biosphere feedback on regional climate in tropical North Africa *Q. J. R. Meteorol. Soc.* **123** 1483–515

Xue Y and Shukla J 1993 The influence of land surface properties on Sahel climate *J. Clim.* **6** 2232–45

Yang Y, Chou S, Li A and Li Z 1992 A study on the water conservation function of the natural forest of Ge's evergreen chinquapin *J. Nat. Resour.* **3** 217–23

Yang Z, Wang J, Ichoku C, Hyer E and Zeng J 2013 Mesoscale modeling and satellite observation of transport and mixing of smoke and dust particles over northern sub-Saharan African region *J. Geophys. Res. Atmos.* **118** 12139–57

Zhang F, Wang J, Ichoku C, Hyer E, Yang Z, Ge C, Su S, Zhang X, Kondragunta S and Kaiser J 2014 Sensitivity of mesoscale modeling of smoke direct radiative effect to the emission inventory: a case study in northern sub-Saharan African region *Environ. Res. Lett.* **9** 075002

Zheng X Y and Eltahir E A B 1997 The response to deforestation and desertification in a model of West African monsoons *Geophys. Res. Lett.* **24** 155–8